Marine Environmental Research 218 (2026) 108016

Contents lists available at ScienceDirect

Marine Environmental Research

journal homepage: www.elsevier.com/locate/marenvrev

Millennial *Posidonia oceanica* reefs reveal contrasting growth trajectories across temporal scales in the Central Mediterranean

Gabriele Rizzuto [a], Federica Paola Cassetti [a,*], Geraldina Signa [a,b,c], Giovanna Cilluffo [a,b,c], Cristina Andolina [a,c], Gianluca Quarta [d], Lucio Calcagnile [d], Salvatrice Vizzini [a,b,c], Agostino Tomasello [a,b,c]

[a] Dipartimento di Scienze della Terra e del Mare, Università degli Studi di Palermo, Palermo, Italy
[b] CoNISMa, Consorzio Nazionale Interuniversitario per le Scienze del Mare, Piazzale Flaminio 9, 00196, Rome, Italy
[c] National Biodiversity Future Center (NBFC), Piazza Marina 61, 90133, Palermo, Italy
[d] CEDAD - Centro di Fisica applicata, Datazione e Diagnostica, Dipartimento di Matematica e Fisica "Ennio De Giorgi", Università del Salento, Italy

ARTICLE INFO

Keywords:
Seagrass ecosystems
Palaeoecological reconstruction
Bioconstruction
Blue-carbon
Climate vulnerability

ABSTRACT

The Mediterranean seagrass *Posidonia oceanica* forms millennia-old biogenic barrier reefs through the vertical growth of rhizomes, roots, and sediments, collectively known as *matte*. It was hypothesised that *P. oceanica* reefs subjected to contrasting hydrodynamic and sedimentary regimes would exhibit divergent long-term accretion trajectories and contemporary growth dynamics, and that millennial-scale *matte* development may reflect present-day plant performance. A multi-proxy analysis on three barrier reefs along the Sicilian coast (Solanto, Maragani and Marsala) was therefore conducted to investigate their long-term development patterns and recent growth dynamics, and to shed light on their vulnerability to climate change. Radiocarbon dating, $\delta^{13}C$ analysis, and lepidochronology revealed contrasting age, growth and sedimentation patterns among the three barrier reefs. The oldest reefs (>1000 years old), Solanto and Maragani, showed contrasting *matte* accretion and rhizome productivity patterns presumably linked to differing hydrodynamics and habitat conditions. The younger and exposed Marsala reef (~600 years old), exhibited the highest *matte* accretion rate, as well as the greatest variability in rhizome speed of growth and primary production likely associated to the highest hydrodynamic regimes coupled with its unique location. Notably, the Solanto reef represents the oldest *P. oceanica* barrier reef dated so far in Italy and ranks among the oldest documented in the Mediterranean Sea. $\delta^{13}C$ values indicated site-specific organic matter preservation and carbon dynamics, with more sheltered reefs showing depleted but variable values over time, indicative of susceptibility to carbon loss. These findings highlight the complex interplay between long-term reef formation and present-day dynamics, providing key insights into the resilience, carbon storage capacity and conservation of shallow *P. oceanica* barrier reefs in the Mediterranean Sea.

1. Introduction

The seagrass *Posidonia oceanica* (L.) Delile is endemic to the Mediterranean Sea, where it forms dense meadows that support ecologically and socioeconomically valuable communities (Vassallo et al., 2013). These meadows rank among the world's most productive ecosystems (Boudouresque et al., 2012; Koopmans et al., 2020; Pergent-Martini et al., 2021) and sustain complex food webs (Vizzini, 2009). Furthermore, *P. oceanica* is the only seagrass species able to build a structure of organic material and sediment known as *matte* (Boudouresque and Meinesz, 1982), through a dense network of roots and rhizomes combined with sediment accumulation (Boudouresque et al., 2012; Gacia and Duarte, 2001).

As the *matte* grows vertically, it can evolve into a unique biogenic structure, called *barrier-reef* (Kendrick et al., 2005). Its development includes two main steps: first, a *fringing reef* is formed (Boudouresque et al., 2012), with leaf tips emerging next to the shore; then, the emersion front advances, moving the edge of the reef away from the coast. Changes in hydrodynamic, temperature and salinity conditions behind the migration front cause the seagrass meadow to die, forming a new lagoon habitat surrounded by a barrier reef of living shoots (Boudouresque et al., 2012) classified in the EUNIS habitat system as the

* Corresponding author.
E-mail address: federicapaola.cassetti@unipa.it (F.P. Cassetti).

https://doi.org/10.1016/j.marenvres.2026.108016
Received 15 January 2026; Received in revised form 16 March 2026; Accepted 20 March 2026
Available online 20 March 2026

"ecomorphosis of barrier-reef *Posidonia oceanica* meadows". *P. oceanica* reefs influence water circulation, sedimentation, and nutrient dynamics, and act as long-term sinks for carbon, nitrogen, phosphorus and trace elements (Apostolaki et al., 2022; Holmer et al., 2019; López-Sáez et al., 2009), thereby playing a critical role in climate change mitigation (Monnier et al., 2021).

P. oceanica reefs have been documented across the Mediterranean Sea, including Spain, France, Tunisia, and Italy, in the past decades (e.g. Calvo et al., 1984; Bonhomme et al., 2015; Hachani et al., 2016; Tomasello et al., 2020; Tomasello et al., 2025) and yet research addressing their development and conservation status is scarce. Some authors investigated the long-term *matte* accretion dynamics using radiocarbon dating (Boudouresque et al., 1980; Mateo et al., 2010; Serrano et al., 2012) but they did not consider the life history traits of the meadow atop, nor these formations have clearly been identified as reefs. Little is known about how millennial-scale *matte* accretion relates to contemporary rhizome growth dynamics. In particular, it remains unclear whether reefs that have accumulated over centuries under specific hydrodynamic and sedimentary regimes maintain comparable growth performance under current climate, or whether long-term development and present-day productivity follow divergent trajectories.

Although the ecological value of the meadows is well recognised (Pergent-Martini et al., 2021; European Commission, 1992; Salomidi et al., 2012), *P. oceanica* barrier reefs are under increasing threat due to human activities (Bonacorsi et al., 2013; Marbà and Duarte, 2010; Pergent et al., 2014). Widespread meadow regression (Litsi-Mizan et al., 2023; Marbà et al., 2014; Montefalcone et al., 2019) and the risk of irreversible damage (Noè et al., 2020; McDonald et al., 2023; Marco-Méndez et al., 2024) underscore the vulnerability of these ecosystems to growing environmental and anthropogenic pressures. Because *matte* accretion occurs over millennia and colonization process is very slow (Kendrick et al., 2005; Boudouresque et al., 1980; Lo Iacono et al., 2008), these reefs have limited resilience to environmental shifts, compromising recovery potential (Tomasello et al., 2025). Maintaining their ecological services requires monitoring of their structural and functional health.

The present study tests the hypothesis that contrasting environmental settings drive distinct long-term accretion patterns and that these historical trajectories may be mirrored by current rhizome growth and productivity. By integrating radiocarbon dating of underlying *matte* deposits with lepidochronological analysis of the living canopy across three Sicilian barrier reefs, this work aims to link millennial-scale reef development with present-day developmental dynamics. Moreover, this study provides the first palaeoecological reconstruction of *P. oceanica* barrier reefs in the Central Mediterranean Sea, including one formation newly documented here.

2. Materials and methods

2.1. Study sites and sampling activities

Sampling was conducted at three *P. oceanica* barrier reefs along the Sicilian coast (Italy, Central Mediterranean), namely Solanto, Maragani, and Marsala (Fig. 1), between October 2018 and February 2021.

Solanto is located approximately 20 km east of Palermo on the northwestern coast of Sicily (38°04′16.5"N, 13°32′19.5"E). The site lies just 2.5 km from the Site of Community Importance (SCI) "Fondali di Capo Zafferano" (ITA020052), which contains a large, well - preserved *P. oceanica* meadow. The area is characterized by a calcarenitic rocky substrate, providing a stable foundation for *P. oceanica* colonization. At

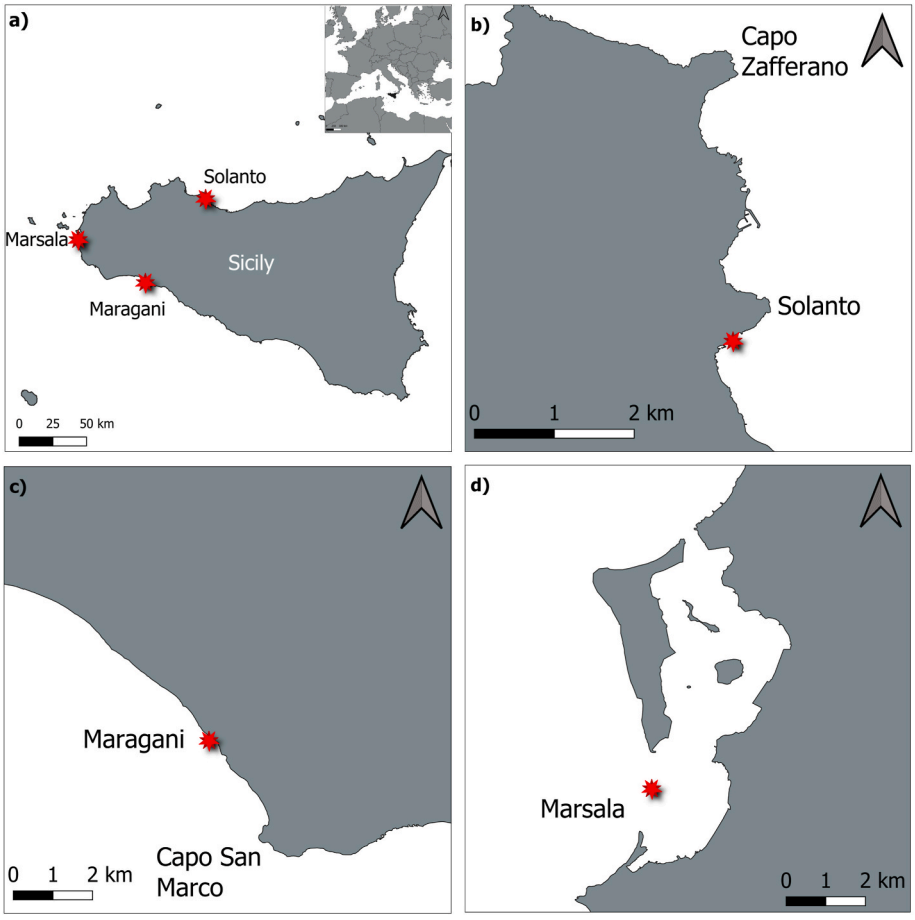

Fig. 1. Study area: a) Sicily, central Mediterranean Sea, and study sites: b) Solanto, c) Maragani, d) Marsala.

this location, the species forms both a barrier reef extending ~500 m and an associated lagoon-like environment towards the coast. This stretch of sea is characterised by low hydrodynamics as it is sheltered from the prevailing winds coming from the west and north by both the Capo Zafferano promontory and the Solanto Point.

Maragani is located within the SCI "Fondali di Capo San Marco - Sciacca" (IT040012). The coastal landscape includes long sandy beaches, rocky promontories, and small pocket beaches. Within this area, *P. oceanica* forms multiple reef structures - six of which extend over a length of approximately 2 km (Tomasello et al., 2020) and supports lagoon-like environments that also host *Cymodocea nodosa* (Ucria) Ascherson and *Zostera noltei* Hornemann (Perzia et al., 2011). For the present study, one reef located off the coastal settlement of Maragani (37°31′41.6"N, 12°59′53.9"E) was selected, extending ~350 m. This reef is subject to pronounced hydrodynamic conditions as is exposed to prevailing winds from the west and south, which promote sediment transport and accumulation within the lagoon (Tomasello et al., 2020).

Marsala is situated on the western coast of Sicily, just outside the southern inlet of the Stagnone di Marsala, a marine coastal basin with lagoon-like features (37°49′59.3"N, 12°26′57.7"E). The area is protected under multiple conservation designations, including the Natura 2000 sites ZSC ITA010001 and ZPS ITA010028. Adjacent to the reef is one of the most extensive and ecologically significant *P. oceanica* meadow in the Mediterranean Sea (Calvo et al., 2010). The site features a well-developed barrier reef, the *Plateau Récifale* (Calvo et al., 1984) located at the interface between lagoonal and open-coast environments under high hydrodynamic regime. This reef is the largest of those under study, extending for ~2 km.

At all sites, three sampling stations were selected covering the total extension of the study reefs (i.e. 100-900 m apart). At each station, two distinct *matte* layers (basal and upper) were sampled by SCUBA divers at depths ranging from 0.5 to 4 m (see Table 1). The basal layer corresponds to the deepest section of the visible *matte*, directly above the underlying substrate, whereas the upper layer corresponds to the overlying *matte* section beneath the living shoots. The thickness of each layer varied among stations and sites according to local reef morphology and is reported in Table 1 as "*Matte* layer thickness". A handsaw was used to cut horizontally approximately 70 cm into the *matte* walls, after carefully removing the outermost layer to avoid any recently deposited organic material. The *matte* samples were then manually extracted and placed into sealed plastic containers, after which they were stored immediately in cooling boxes to preserve their physical and chemical integrity until further processing. Total *matte* thickness was also determined as the vertical distance between the reef top and the basal *matte* boundary.

Approximately 60 *P. oceanica* shoots per site with orthotropic (vertical) rhizomes were randomly collected from the top of each reef (~20 per station) at depths ranging from 0.1 to 1.3 m, for lepidochronological analysis. The bathymetric depths of the basal and intermediate *matte* samples and the reef top were recorded at each station using a depth gauge. All samples were stored in seawater-filled cooling boxes in the dark and transported to the laboratory where they were stored at −20 °C for subsequent analysis.

2.2. Paleodating

The age of the *matte* samples was estimated by calculating their ^{14}C content through Accelerator Mass Spectrometry (AMS). One sample per layer per station was analysed. First, a pretreatment was applied to remove extraneous material from samples, using both mechanical and chemical (acid-alkaline-acid) treatments. Samples were combusted at 900 °C in an oxidative environment to produce carbon dioxide gas, which was then reduced with hydrogen and iron dust as catalysts to form graphite. Radiocarbon concentration was determined by comparing the measured currents of ^{12}C, ^{13}C, and ^{14}C with standard values obtained from Sucrose C_6 samples provided by the International Atomic Energy Agency (IAEA). The Conventional Radiocarbon Age was corrected for isotopic fractionation using the $\delta^{13}C$ value calculated by the Accelerator. Oxalic acid standards from the National Institute of Standards and Technology (NIST) were used as an analytical control. The experimental error in radiocarbon dating was calculated considering both the data scatter around the mean and the standard error of ^{14}C readings. Age was expressed in years before present (BP) using the "Libby half-life" of 5568 years.

2.3. Lepidochronological analysis

Lepidochronological analysis was conducted on orthotropic rhizomes with intact basal portion collected from each site (Tomasello et al., 2016) following the method described by Pergent et al. (1989). Before analysis, the samples were rinsed with tap water to remove sediment and debris. Briefly, *P. oceanica* scales were gently removed from the rhizomes, arranged on a bench, sectioned 10 mm from their base (insertion point on the rhizome), and examined with a micrometric lens to estimate their thickness, in order to detect each lepidochronological cycle corresponding to one year of growth (lepidochronological year), delimited by two consecutive minimum thicknesses along the rhizome (Pergent et al., 1989). The age of each shoot was determined by counting the lepidochronological years from the apex of the rhizome to its base. Rhizome segments corresponding to each lepidochronological year were excised with a scalpel, and their length was measured with a calliper. Rhizome segments were also oven-dried at 105 °C for 24 h and

Table 1
Sampling design and characteristics of the *P. oceanica* barrier reefs at the three study sites.

Site	Station	Reef top depth (m)	Basal *matte* depth (m)	Total *matte* thickness (m)	*Matte* sampling depth (m)	*Matte* layer thickness (m)	*Matte* layer name
Solanto	1	1.0	4.0	3.0	4.0	1.5	Basal
					2.5	1.5	Upper
	2	1.3	3.5	2.2	3.5	1.5	Basal
					2.0	0.7	Upper
	3	1.0	2.6	1.6	2.6	0.7	Basal
					1.9	0.9	Upper
Maragani	1	0.3	1.2	0.9	1.2	0.7	Basal
					0.5	0.2	Upper
	2	0.1	1.1	1.0	1.1	0.6	Basal
					0.5	0.4	Upper
	3	0.4	1.7	1.3	1.7	1.0	Basal
					0.7	0.3	Upper
Marsala	1	1.0	2.8	1.8	2.8	1.1	Basal
					1.7	0.7	Upper
	2	0.8	2.5	1.7	2.5	1.0	Basal
					1.5	0.7	Upper
	3	0.3	2.3	2.0	2.3	0.9	Basal
					1.4	1.1	Upper

weighed. The length of each annual segment was used to estimate rhizome vertical speed of growth (mm year^{-1}), while the dry weight of each annual segment was used, as rhizome primary production (mg dry weight year^{-1}). Moreover, the total length and weight of each rhizome were calculated as the sum of the length and weight values recorded (for further details see Tomasello et al., 2016).

2.4. Data analysis

2.4.1. Long-term growth (matte accretion)

Radiocarbon data were filtered to remove stratigraphic inconsistencies potentially arising from erosion, redeposition, or organic contamination (Serrano et al., 2012; Mateo et al., 1997). In addition, samples younger than 1950 AD (n = 3: 2 from Solanto, 1 from Maragani) were excluded as their age is too recent to yield reliable radiocarbon-based estimates.

The radiocarbon age obtained for each sampled layer (basal and upper, see Table 1) was used to reconstruct the accretion history of the corresponding vertical section of the *matte*. The basal layer corresponds to the lowest stratigraphic unit of the *matte*, directly overlying the surrounding substrate, whereas the upper layer represents the stratigraphic unit lies that immediately the living canopy. The accretion time of each layer was calculated using the age difference between the two dated layers at the same station. Specifically, basal layer accretion time corresponds to the time elapsed between the basal sample age and the upper sample age, whereas upper layer accretion time corresponds to the time between the upper sample age and the present. *Matte* accretion rates (mm year^{-1}) were then calculated by dividing the measured layer thickness by its corresponding accretion time (see Table 2).

2.4.2. Short-term growth (rhizome speed of growth, length and weight)

To avoid the effect of no closed lepidochronological year (only one thinnest scale was present), the last segment at the top of each rhizome was excluded from data analyses. Moreover, the most recent annual rhizome segments (the last two) were excluded from the analysis, because they were still growing at the time of sampling (see Tomasello et al., 2016 and references therein). After filtering, a total of 247 rhizome segments were retained and analysed across the three sites (Table 4). Mean total length and weight of the rhizomes across the sampling sites were then compared against reference growth charts developed by Tomasello et al. (2016) to account for the confounding effect of shoot age (Bacci et al., 2025; Tomasello et al., 2007). This classification procedure is based on percentile ranges, describing the distribution of rhizome length and weight as a function of shoot age and depth. Analogous to growth charts used in human biometrics, these percentiles provide age-dependent reference growth values against which to compare the measured growth within a sampled population. Each sampled rhizome was assigned to a percentile class (<5th, 5th–25th, 25th–50th, ≥50th) according to its position relative to this reference dataset. Lower percentiles indicate reduced growth performance compared to the reference population, whereas higher percentiles reflect above-average growth. Rhizome measurements falling within each percentile range were compared among sites (Solanto, Maragani, Marsala) using chi-square tests of independence. Correspondence analysis (CA) biplots visualized the multivariate relationships between sites and growth percentiles, with dimensions representing the relative contribution of each variable to overall variance. All statistical analyses were performed in R (v 4.3.1), with significance set at $p < 0.05$. All site differences were assessed using a non-parametric Kruskal-Wallis test, followed by Dunn test (adjusted $p < 0.025$).

Table 2
Accretion rate (mm/year) provided by the current study and scientific literature.

Site/Region	Accretion Rate (mm/year)	Source/Reference
Marsala (Basal layer)	6.6 ± 6.0	This study (Sicily)
Solanto (Basal layer)	3.5 ± 3.7	This study (Sicily)
Maragani (Basal layer)	2.0 ± 1.2	This study (Sicily)
Marsala (Upper layer)	2.2 ± 1.2	This study (Sicily)
Solanto (Upper layer)	1.7 ± 0.4	This study (Sicily)
Maragani (Upper layer)	0.6 ± 0.1	This study (Sicily)
Cala Culip (Spain),	2.3	Romero et al. (1994)
Port Lligat Bay (NE Iberian Peninsula)	1.12 ± 0.39	López-Sáez et al. (2009)
Culip, Port Lligat, Medes, Campello, Tabarca and Ischia	1.75 ± 1.18	Mateo et al. (1997)
Port Lligat Bay	1.1	Lo Iacono et al. (2008); Mateo et al. (2010)
Corsica (France)	~0.6	Boudouresque et al. (1980)
Port Lligat Bay	1.3	Serrano et al. (2012)

3. Results

3.1. Long-term matte development and radiocarbon dating

Radiocarbon analysis revealed distinct, centennial-scale *matte* development across the three *Posidonia oceanica* reefs, with notable variability between the basal and upper layers (Tables 2 and 3). Solanto showed the oldest basal deposits, followed by Maragani, then Marsala. The upper layers were consistently younger at all sites, though the magnitude of the age difference between the basal and upper layers varied between sites. In contrast, the accretion time of the layers was overall lower in the basal layers than in their upper counterparts. The estimated vertical accretion rates of the *matte* also varied across sites and layers (Table 3). Solanto showed moderate growth in the deeper basal layer of the *matte*, contrasting with the slower accumulation at Maragani and the notably faster deposition at Marsala. All reefs exhibited a substantially reduced accretion rate in the upper layer, with Solanto and Marsala maintaining slightly higher rates than Maragani.

The $\delta^{13}C$ values revealed distinct organic matter dynamics across sites and *matte* layers (Table 3). The basal layers showed more depleted values in Solanto, followed by Maragani and Marsala. The upper layers showed a different spatial pattern: Solanto, and, to a lesser extent, Maragani exhibited pronounced ^{13}C enrichment compared to Marsala. Furthermore, Marsala showed more consistent $\delta^{13}C$ values across layers than the other reefs.

3.2. Rhizome growth and productivity

Lepidochronological analysis also revealed clear site-specific differences in shoot development and productivity (Table 4), although these differed from the spatial trends described above. Marsala exhibited the youngest shoots, followed by Solanto and Maragani with the oldest shoots. At the same time, Marsala displayed intermediate values for all the other morphometric traits and productivity metrics, with Solanto showing the smallest rhizomes with the lowest biomass and Maragani the largest rhizomes with the highest biomass.

Boxplots showed highly significant differences in both speed of growth and primary production of rhizomes among sites (Fig. 2). Solanto showed consistently lower values, with growth and primary production approximately half those of Maragani. Marsala displayed intermediate performance for both metrics, though with greater variability in both speed of growth and primary production. Maragani maintained unequivocal dominance in both speed of growth (~10 mm/yr) and productivity (~100 mg/yr).

3.3. Growth performance relative to reference percentiles

When compared to the reference growth percentiles (Table 5), the *P. oceanica* rhizomes from Solanto consistently ranked in the lowest percentiles for both length and weight. (<5th), while Maragani exhibited a tendency toward longer rhizomes (25th-50th percentiles). Marsala

Table 3
Results of radiocarbon and stable isotope analyses across sites and *matte* layers (basal, upper). Mean ± SD. N = number of replicates. * datation not available for 1 replicate; ** stratigraphic inconsistencies in 1 replicate.

Site	*Matte* layer	N	Age BP (years)	Layer accretion time (years)	*Matte* accretion rate (mm/year)	$\delta^{13}C$ (‰)
Solanto	Basal	3	1210.0 ± 247.6	509.3 ± 274.2	3.5 ± 3.7	−17.3 ± 3.0
	Upper	2**	723.5 ± 16.3	723.5 ± 16.3	1.7 ± 0.4	−11.7 ± 3.0
Maragani	Basal	2*	1033.5 ± 306.2*	425.5 ± 109.6	2.0 ± 1.2	−14.1 ± 3.2
	Upper	2*	609.0 ± 196.6	609.0 ± 196.6	0.6 ± 0.1	−11.0 ± 3.7
Marsala	Basal	3	632.3 ± 168.5	214.8 ± 127.4	6.6 ± 6.0	−13.7 ± 3.3
	Upper	2*	502.0 ± 4.2	502.0 ± 4.2	2.2 ± 1.2	−13.8 ± 3.8

Table 4
Morphometric traits estimated by lepidochronology of orthotropic rhizomes. Mean ± SD. N = total number of rhizome segments. Results of the non-parametric Kruskal-Wallis test among sites are also showed.

Site	N	Shoot age (years)	Total length (mm)	Total weight (mg dw)
Solanto	58	7.0 ± 3.9	32.4 ± 17.0	359.1 ± 208.0
Maragani	72	10.1 ± 6.4	106.1 ± 70.1	1022.9 ± 605.9
Marsala	117	5.8 ± 3.1	43.7 ± 29.5	533.7 ± 384.5
KW p-value		<0.001	<0.001	<0.001

showed an intermediate pattern, with a noticeable proportion of rhizomes at both the lowest and intermediate lengths intermediate percentiles, indicating a bimodal distribution. Rhizome weight distributions followed a similar site-specific trends pattern ($\chi^2 = 22.813$ for length, 15.82 for weight; $p < 0.0008$ and 0.015 respectively). Statistical tests confirmed that these differences were highly significant, with Maragani again showing significantly greater representation in the upper percentiles, which reinforced the distinct rhizome growth profiles observed at each site.

Correspondence analysis (CA) biplots revealed clear distinctions in the growth profiles of *P. oceanica*, particularly regarding Dim1. This dimension captured most of the variance in both rhizome length (82%) and weight (58.6%) (Fig. 3). In more detail, rhizome length percentiles were arrayed along Dim1 reflecting differences among sites. Solanto was strongly aligned with the lowest growth class (0th–5th percentile), while Maragani was positioned at the opposite end and associated with the 25th-50th percentiles, indicating its tendency towards longer rhizomes. Marsala fell between these extremes, positioning next to the origin of the biplot and thus representing intermediate values; a similar pattern was observed for rhizome weight along Dim1. Once again, Maragani was clearly distinct from Solanto and Marsala, suggesting a consistent pattern of biomass production. The distinct positioning of Maragani

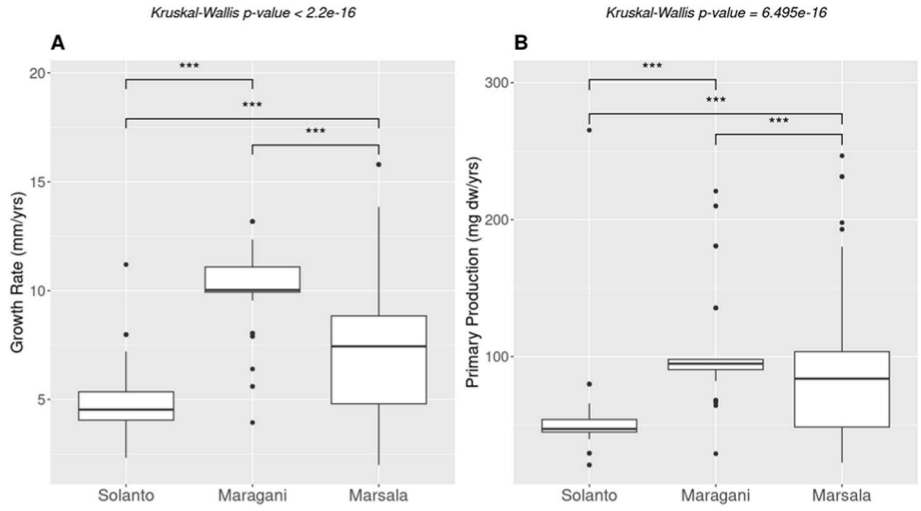

Fig. 2. Comparison of (A) speed of growth (mm/year) and (B) primary production of *P. oceanica* rhizome segments expressed as dry weight (mg dw/year) across the study sites: Solanto (n = 58), Maragani (n = 72), and Marsala (n = 117). Boxplots show median values (lines), interquartile ranges (whiskers), and outliers (dots). Results of the non-parametric Kruskal-Wallis test among sites followed by pairwise comparisons are also showed. Significance levels are indicated as: *p < 0.05, **p < 0.01, ***p < 0.001.

Table 5
Individual counts and percentage of *P. oceanica* rhizomes distributed along percentiles derived from rhizome length (A) and rhizome weight (B) reference growth charts, across the study sites.

Site	A) Rhizome length				B) Rhizome weight			
	<5th	5th-25th	25th-50th	50th-95th	<5th	5th-25th	25th-50th	50th-95th
Solanto	15	2	1	0	10	5	0	1
Maragani	3	4	9	0	2	11	0	3
Marsala	19	11	5	2	12	12	5	8
% Solanto	40.5	11.8	6.7	0	41.7	18.8	0	8.3
% Maragani	8.1	23.5	60	0	8.3	39.3	0	25
%Marsala	51.4	64.7	33.3	100	50	42.8	100	66.7
	$\chi^2 = 22.813$, Df = 6, P < 0.0008				$\chi^2 = 15.82$, Df = 6, P < 0.015			

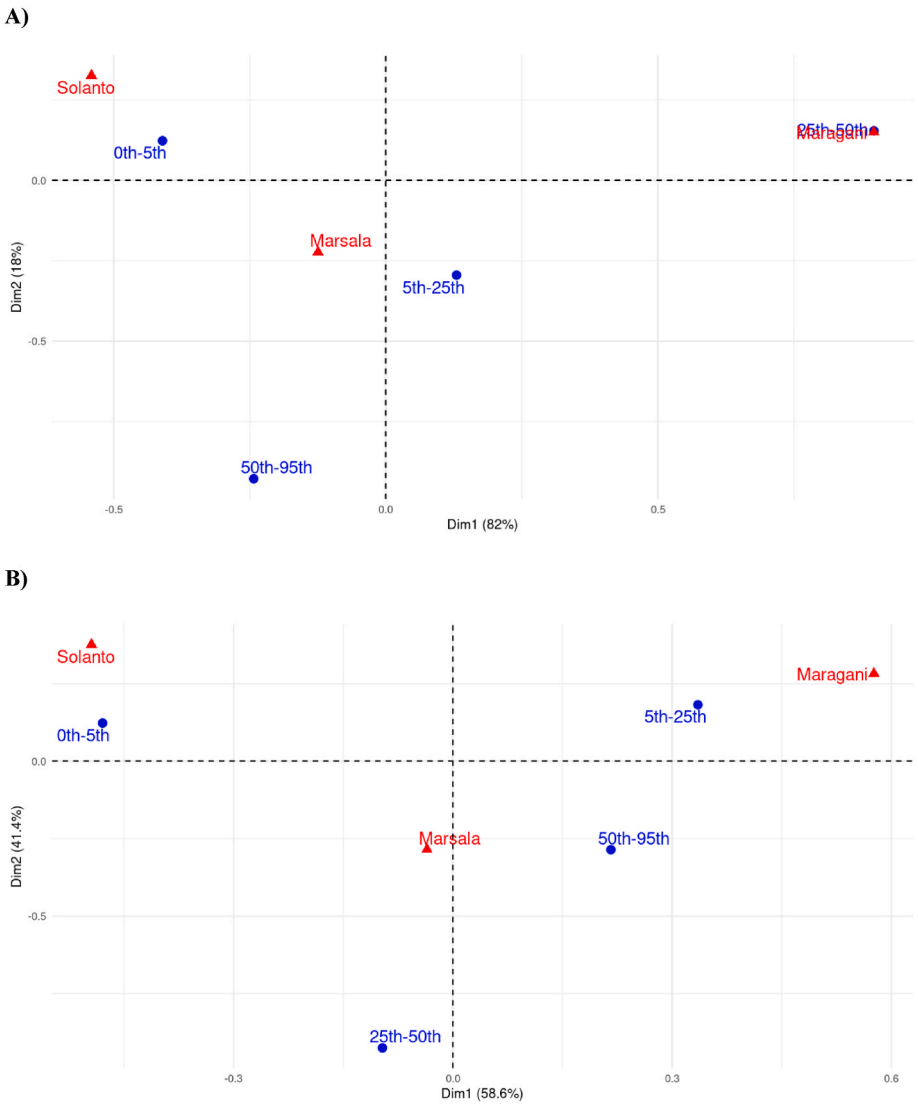

Fig. 3. Correspondence Analysis biplots for *P. oceanica* rhizome length (A) and rhizome weight (B). Sites are represented in red, while percentiles derived from growth charts in blue. Dim1 = Dimension 1; Dim2 = Dimension 2. (For interpretation of the references to colour in this figure legend, the reader is referred to the Web version of this article.)

along the dominant axis in both analyses underscores its unique growth conditions compared to the other two sites.

4. Discussion

Radiocarbon and morphometric dating provided insight into the long- and short-term growth dynamics of three *P. oceanica* barrier reef meadows along the Sicilian coast in the central Mediterranean. Although similar approaches have been applied in other regions (e.g. Mateo et al., 2010), this study is the first to attempt a paleoecological reconstruction of *P. oceanica* reefs, by assessing the dynamics of both the dead and living components of the reef.

Matte thickness varied between about 1 and 3 m across the three study sites, consistent with previous observations of *P. oceanica* reef structures in other Mediterranean sites (Monnier et al., 2021). The long-term vertical accretion rates of the reefs in the present study, estimated by dividing the radiocarbon age by the *matte* thickness, were overall consistent with those reported elsewhere in the Mediterranean Sea using different approaches (Table 2 and references therein). Although core-based stratigraphy provides a finer resolution (Boudouresque et al., 1980), the methodological approach used in this study still yields reliable results. The present study provides, to the best of our knowledge, the first radiocarbon-based paleoecological reconstruction of *P. oceanica* reefs in the central Mediterranean. Results show that the Solanto *matte* formation constitutes the oldest documented *P. oceanica* barrier reef in Italy, since other *matte* structures have not previously been interpreted as reefs (Mateo et al., 1997).

The moderate accretion rate recorded at Solanto, which is intermediate between the lowest rate recorded at Maragani and the highest rate at Marsala, reflects distinct long term developmental trajectories among the reefs. At Solanto, the least exposed site, the long-term reef accretion appears to be the result of sustained *matte* formation under relatively low hydrodynamic conditions, coupled with limited but consistent sediment deposition over time. Such depositional conditions favour gradual sediment accumulation and long-term carbon storage (Gaglianone et al., 2017; Serrano et al., 2016) also explaining the highest *matte* height and age found in this reef. At Maragani, the higher exposure may have promoted the resuspension and redistribution of allochthonous sediment within the reef over time, rather than vertical *matte* accretion. This would explain the lowest accretion rates and thickness compared with Solanto and Marsala, despite the reef's millennial age. This condition may also have enhanced rhizome

elongation as *P. oceanica* adjusts to periodic burial (Marbà and Duarte, 1994).

In contrast, the highest long-term *matte* accretion rate was found in Marsala, which is the most exposed site, with the youngest reef. This can be linked to its unique location at the interface between the "Stagnone di Marsala" lagoon and the open sea, as well as in front of the largest *P. oceanica* meadow in Sicily - and one of the most extensive in the Mediterranean (Nguyen et al., 2023). While the "Stagnone di Marsala" lagoon provides an abundant sediment supply and an efficient depositional environment (Agnesi et al., 1993), the adjacent *P. oceanica* meadow, which extend over an area of approximately 1090 ha in front of about 500 m of coastline (compared to 83 and 43 ha at Maragani and Solanto respectively EMODnet (European Marine Observation and Data Network), 2025), may have significantly dampened local hydrodynamics by reducing near-bed flow and turbulence, thereby enhancing sediment retention and promoting reef accretion stability.

Seagrass meadows act as efficient carbon sinks due to their ability to trap and preserve organic matter in anoxic sediments (Kennedy et al., 2010; Mazarrasa et al., 2015). Across the three sites, $\delta^{13}C$ values confirm distinct depositional dynamics. The most exposed reef, Marsala, showed consistently higher $\delta^{13}C$ values than the other reefs, suggesting enhanced *in situ* carbon burial driven by rapid sediment deposition and limited decomposition. In contrast, the less exposed Solanto reef displayed more depleted $\delta^{13}C$ signatures, consistent with lower sedimentation rates and a relatively greater contribution of allochthonous organic matter. The Maragani site, which has intermediate hydrodynamics, exhibited intermediate $\delta^{13}C$ values reflecting moderate sediment resuspension and the partial burial of seagrass-derived organic matter (Lavery et al., 2013; Bouillon and Boschker, 2006).

Despite these site-specific differences, a comparable temporal pattern emerged across the three reefs when comparing the two dated layers. The basal layers, representing the earliest phase of reef development but not necessarily half of its formation time, showed accretion rates two to three times higher than those of the upper layers. This decrease in accretion rate has previously been observed in ancient *mattes* along the Corsican coast (Boudouresque et al., 1980) and may likely reflect a progressive slowdown in vertical *matte* accretion potentially associated with sea-level stabilization, reduced sediment availability, and self-limiting feedback linked to higher reef maturity (Monnier et al., 2021). Furthermore, $\delta^{13}C$ values generally increase from the basal to upper layers, suggesting that organic matter gradually breaks down and is recycled as it becomes buried. This depth-related pattern highlights the key role of sediment accumulation in controlling long-term carbon storage and indicates why some reefs may be more vulnerable to carbon loss than others (Serrano et al., 2016; Mazarrasa et al., 2018).

Interestingly, clear differences along the reef vertical profile were evident when comparing vertical growth of living *P. oceanica* rhizomes with long-term reef accretion rate. Present-day rhizome elongation rates are approximately one to five times higher than the accretion rates found in the basal, older *matte* layers and up to seventeen times higher than accretion rates in the upper *matte* layers at Maragani. This discrepancy indicates that much of the organic material produced by rhizomes has not been preserved within the *matte*. Missing necromass likely reflects episodic storm-driven detachment and sediment remobilization, which have been documented along southern Sicilian coasts as "reef cemeteries" of stranded *P. oceanica matte* blocks (Tomasello et al., 2025), highlighting a high reef vulnerability (Marbà and Duarte, 2010; Mazarrasa et al., 2018). Additionally, repeated sediment reworking followed by recolonization may have contributed to discontinuities in accretion (Mateo et al., 1997, 2010; Marbà et al., 1996; Gera et al., 2014). These processes are therefore intrinsic to *P. oceanica* reef development and must be considered when interpreting long-term accretion, carbon storage, and climate vulnerability (Marco-Méndez et al., 2024; Oprandi et al., 2020).

Rhizome growth dynamics reflect a complex interplay between meadow age, sediment deposition, and local habitat conditions. Vertical rhizome elongation across all sites indicates ongoing sediment accretion, consistent with the role of *P. oceanica* in coastal stabilization and geomorphological structuring (Manzanera et al., 2011; Potouroglou et al., 2017). However, in the oldest reef at Solanto, reduced rhizome elongation and thickening were evident. This aligns with local patterns of low productivity in aging shoots (Tomasello et al., 2016) and is likely exacerbated by shallow depth-related stressors such as sediment resuspension, wave exposure, and elevated temperatures (Nguyen et al., 2023). Consequently, even ancient meadows show diminished capacity as carbon sinks and sediment stabilizers, highlighting their vulnerability to contemporary anthropogenic pressures. In contrast, Maragani, although slightly younger, displayed higher rhizome growth and productivity, suggesting that local depositional conditions favour plant vigour and persistence at decadal scales. Cooler temperatures along southern Sicilian coasts may further enhance growth at shallow depths under favourable sedimentation regimes (De Falco et al., 2008). The youngest reef, Marsala, occupied an intermediate position in growth and productivity, exhibiting the highest reef accretion rate and greater variability in individual rhizome performance. The coexistence of vigorous and weaker individuals indicates a system still capable of recovery but showing early signs of localized stress (McDonald et al., 2023).

Caution is required when applying percentile-based growth frameworks (Tomasello et al., 2016) to extremely shallow *P. oceanica* reefs. These models were developed primarily from deeper meadows (4 – 32 m) that experience different light regimes, hydrodynamics, and sediment dynamics. Shallow meadows can exhibit distinct growth strategies under higher wave energy, temperature, and light exposure (Montefalcone et al., 2019), highlighting the need for new reference growth charts for depths lower than 4 m to more accurately interpret growth trends and ecological function in these reef environments.

These findings provide insight into the future trajectory of *P. oceanica* barrier systems under climate change. Although millennial *matte* accumulation demonstrates long-term persistence, reduced contemporary rhizome elongation suggests that historical resilience does not necessarily translate into present-day robustness, potentially jeopardizing the future stability of these structures under changing climate scenarios. As the Mediterranean region is experiencing increasing storm intensity and thermal stress (Napolitano et al., 2025; Jangir et al., 2024), the capacity of reefs to maintain vertical accretion and preserve carbon stocks may depend on the balance between sediment supply and biological production. Reefs are particularly vulnerable to extreme climate events, facing catastrophic losses due to detachment and stranding of *matte* blocks (Tomasello et al., 2025), and resilience to disturbances may depend on the maintenance of their accretion speed. Moreover, reefs where present-day rhizome elongation remains sufficient to offset erosion may retain their structural and carbon-storage functions, whereas systems showing reduced morphometric performance could become increasingly vulnerable to *matte* destabilization and carbon remobilization. The integration of radiocarbon-based accretion histories with lepidochronological growth assessment represents a valuable framework for identifying resilient versus potentially vulnerable reefs and support conservation planning under environmental change.

5. Conclusions

This study provides the first integrated assessment of the long-term development and recent growth dynamics of *P. oceanica* reefs in the central Mediterranean Sea by combining radiocarbon dating, lepidochronology and stable carbon isotope analyses. The three reefs studied are long-lived biogenic structures formed through centuries of *matte* accretion exhibiting distinct age and growth dynamics shaped by environmental gradients and local stressors. Notably, the Solanto reef ranks among the oldest documented in the Mediterranean Sea. The older and more sheltered reef (Solanto) showed carbon dynamic characterized by more depleted $\delta^{13}C$ values but contrasting sediment accumulation

rates and growth patterns, challenging the assumption that reef age alone predicts seagrass vitality. Conversely, the younger and more exposed reef (Marsala) exhibited more consistent growth, productivity, and carbon dynamics, indicating lower vulnerability to ongoing climatic stressors and underscoring the key role of local conditions in reef resilience. Collectively, these findings demonstrate how millennia of accretion can be undermined by contemporary stressors, threatening reef persistence. Monitoring growth percentile trends over time could provide early warnings of decline and guide targeted conservation efforts. This study confirms the usefulness of integrating paleoecological, lepidochronological and isotopic proxies to capture the complex interplay between historical development and current ecosystem functioning. As critical carbon sinks and coastal stabilizers, *P. oceanica* reefs face increasing risks from erosion, storms, and anthropogenic pressures, highlighting the urgent need for conservation strategies informed by long-term perspectives.

CRediT authorship contribution statement

Gabriele Rizzuto: Writing – review & editing, Writing – original draft, Formal analysis, Data curation, Conceptualization. **Federica Paola Cassetti:** Writing – review & editing, Writing – original draft, Investigation. **Geraldina Signa:** Writing – review & editing, Writing – original draft, Conceptualization. **Giovanna Cilluffo:** Writing – review & editing, Supervision, Formal analysis, Data curation. **Cristina Andolina:** Writing – review & editing, Writing – original draft, Conceptualization. **Gianluca Quarta:** Writing – review & editing, Investigation. **Lucio Calcagnile:** Writing – review & editing, Investigation. **Salvatrice Vizzini:** Writing – review & editing, Supervision, Methodology, Funding acquisition, Conceptualization. **Agostino Tomasello:** Writing – review & editing, Supervision, Methodology, Funding acquisition, Conceptualization.

Funding

This study was supported by the European Union - Next-Generation EU through the Italian Ministry of University and Research under PNRR - M4C2 – I1.3 Projects: RETURN “multi-Risk sciEnce for resilient commUnities undeR a changiNg climate” Extended Partnership (CUP B73C22001220006) and NBFC “National Biodiversity Future Center” CUP B73C22000790001- SPOKE 1. The work was also funded by the European Regional Development Fund (INTERREG Italia–Malta) under the project BESS “Pocket Beach Management and Remote Surveillance System”.

Declaration of competing interest

The authors declare that they have no known competing financial interests or personal relationships that could have appeared to influence the work reported in this paper.

Data availability

Data will be made available on request.

References

Agnesi, V., Macaluso, T., Orrù, P., Ulzega, A., 1993. Paleogeografia dell’arcipelago delle Egadi (Sicilia) nel Pleistocene sup.-olocene. Naturalista Siciliano XVII (1-2), 3–22. S. IV.

Apostolaki, E.T., Caviglia, L., Santinelli, V., Cundy, A.B., Tramati, C.D., Mazzola, A., Vizzini, S., 2022. The importance of dead seagrass (*Posidonia oceanica*) matte as a biogeochemical sink. Front. Mar. Sci. 9, 861998. https://doi.org/10.3389/fmars.2022.861998.

Bacci, T., Scardi, M., Tomasello, A., Valiante, L.M., Piazzi, L., Calvo, S., et al., 2025. Long-term response of *Posidonia oceanica* meadow restoration at the population and plant level: implications for management decisions. Restor. Ecol. 33, e14360. https://doi.org/10.1111/rec.14360.

Bonacorsi, M., Pergent-Martini, C., Bréand, N., Pergent, G., 2013. Is *Posidonia oceanica* regression a general feature in the Mediterranean Sea? Mediterr. Mar. Sci. 14 (1), 193–203. https://doi.org/10.12681/mms.334.

Bonhomme, D., Boudouresque, C.F., Astruch, P., Bonhomme, J., Bonhomme, P., Goujard, A., Thibaut, T., 2015. Typology of the Reef Formations of the Mediterranean Seagrass *Posidonia oceanica*, and the Discovery of Extensive Reefs in the Gulf of Hyères (Provence, Mediterranean), 29. Scientific Report of the Port-Cros National Park, pp. 41–73.

Boudouresque, C.-F., Meinesz, A., 1982. Découverte De L’Herbier De Posidonies, 4. Cahiers du Parc National de Port-Cros, pp. 1–79.

Boudouresque, C.F., Thommeret, J., Thommeret, Y., 1980. Sur la découverte d'un bioconcrétionnement fossile intercalé dans l'herbier à *Posidonia oceanica* de la baie de Calvi (Corse). Journees d'etudes sur la Systematique Evolutive et la Biogeographie en Mediterranee/1980 139–142.

Boudouresque, C.F., Bernard, G., Bonhomme, P., Charbonnel, E., Diviacco, G., Meinesz, A., Pergent, G., Pergent-Martini, C., Ruitton, S., Tunesi, L., 2012. Protection and Conservation of *Posidonia oceanica* Meadows. RAMOGE and RAC/SPA publisher, Tunis, pp. 1–202. N° 2-905540-31-1.

Bouillon, S., Boschker, H.T.S., 2006. Bacterial carbon sources in coastal sediments: a cross-system analysis based on stable isotope data of biomarkers. Biogeosciences 3 (2), 175–185. https://doi.org/10.5194/bg-3-175-2006.

Calvo, S., Fradà, Orestano C., 1984. L’herbier de *Posidonia oceanica* des cotes siciliennes: les formations Re'cifales du Stagnone. In: Boudouresque, C.F., Jeudy de Grissac, A., Olivier, J. (Eds.), International Workshop on *Posidonia oceanica* Beds, 1. GIS Posidonie publ, Fr., pp. 29–37

Calvo, S., Tomasello, A., Di Maida, G., Pirrotta, M., Cristina Buia, M., Cinelli, F., Cormaci, M., Furnari, G., Giaccone, G., Luzzu, F., Mazzola, A., 2010. Seagrasses along the Sicilian coasts. Chem. Ecol. 26 (S1), 249–266. https://doi.org/10.1080/02757541003636374.

De Falco, G., Baroli, M., Cucco, A., Simeone, S., 2008. Intrabasinal conditions promoting the development of a biogenic carbonate sedimentary facies associated with the seagrass *Posidonia oceanica*. Cont. Shelf Res. 28 (6), 797–812. https://doi.org/10.1016/j.csr.2007.12.014.

EMODnet (European Marine Observation and Data Network), 2025. EMODnet portal. https://emodnet.ec.europa.eu/en/seabed-habitats.

European Commission, 1992. *Council directive 92/43/EEC on the conservation of natural habitats and of wild fauna and flora. Off. J. Europ. Commun. L206, 7–50. http://data.europa.eu/eli/dir/1992/43/oj.

Gacia, E., Duarte, C.M., 2001. Sediment retention by a Mediterranean *Posidonia oceanica* meadow: the balance between deposition and resuspension. Estuar. Coast Shelf Sci. 52 (4), 505–514. https://doi.org/10.1006/ecss.2000.0753.

Gaglianone, G., Brandano, M., Mateu-Vicens, G., 2017. The sedimentary facies of *Posidonia oceanica* seagrass meadows from the central Mediterranean Sea. Facies 63 (4), 28. https://doi.org/10.1007/s10347-017-0511-2.

Gera, A., Pagès, J.F., Arthur, R., Farina, S., Roca, G., Romero, J., Alcoverro, T., 2014. The effect of a centenary storm on the long-lived seagrass *Posidonia oceanica*. Limnol. Oceanogr. 59 (6), 1910–1918. https://doi.org/10.4319/lo.2014.59.6.1910.

Hachani, M.A., Ziadi, B., Langar, H., Sami, D.A., Turki, S., Aleya, L., 2016. The mapping of the *Posidonia oceanica* (L.) delile barrier reef meadow in the southeastern Gulf of Tunis (Tunisia). J. Afr. Earth Sci. 121, 358–364. https://doi.org/10.1016/j.jafrearsci.2016.05.030.

Holmer, M., 2019. Productivity and biogeochemical cycling in seagrass ecosystems. In: Perillo, G.M.E., Wolanski, E., Cahoon, D.R., Hopkinson, C.S. (Eds.), Coastal Wetlands: an Integrated Ecosystem Approach, second ed. Elsevier, pp. 539–563. https://doi.org/10.1016/B978-0-444-63893-9.00013-7.

Jangir, B., Mishra, A.K., Strobach, E., 2024. The interplay between medicanes and the Mediterranean Sea in the presence of sea surface temperature anomalies. Atmos. Res. 310, 107625. https://doi.org/10.1016/j.atmosres.2024.107625.

Kendrick, G.A., Marbà, N., Duarte, C.M., 2005. Modelling formation of complex topography by the seagrass *Posidonia oceanica. Estua*rine. Coast. Shelf Sci. 65 (4), 717–725. https://doi.org/10.1016/j.ecss.2005.07.007.

Kennedy, H., Beggins, J., Duarte, C.M., Fourqurean, J.W., Holmer, M., Marbà, N., Middelburg, J.J., 2010. Seagrass sediments as a global carbon sink: isotopic constraints. Glob. Biogeochem. Cycles 24 (4). https://doi.org/10.1029/2010GB003848. GB4026.

Koopmans, D., Holtappels, M., Chennu, A., Weber, M., de Beer, D., 2020. High net primary production of Mediterranean seagrass (*Posidonia oceanica*) meadows determined with aquatic eddy covariance. Front. Mar. Sci. 7, 118. https://doi.org/10.3389/fmars.2020.00118.

Lavery, P.S., Mateo, M.Á., Serrano, O., Rozaimi, M., 2013. Variability in the carbon storage of seagrass habitats and its implications for global estimates of blue carbon ecosystem service. PLoS One 8 (9), e73748. https://doi.org/10.1371/journal.pone.0073748.

Litsi-Mizan, V., Efthymiadis, P.T., Gerakaris, V., Serrano, O., Tsapakis, M., Apostolaki, E. T., 2023. Decline of seagrass (*Posidonia oceanica*) production over two decades in the face of warming of the Eastern Mediterranean Sea. New Phytol. 239 (6), 2126–2137. https://doi.org/10.1111/nph.19084.

Lo Iacono, C., Mateo, M.A., Gràcia, E., Guasch, L., Carbonell, R., Serrano, L., Serrano, O., Danobeitia, J.J., 2008. Very high-resolution seismo-acoustic imaging of seagrass meadows (Mediterranean sea): implications for carbon sink estimates. Geophys. Res. Lett. 35 (18), L18601. https://doi.org/10.1029/2008GL034773.

López-Sáez, J.A., López-Merino, L., Mateo, M.A., Serrano, O., 2009. Palaeoecological potential of the marine organic deposits of *Posidonia oceanica*: a case study in the NE Iberian peninsula. Palaeogeogr. Palaeoclimatol. Palaeoecol. 271, 215–224. https://doi.org/10.1016/j.palaeo.2008.10.020.

Manzanera, M., Alcoverro, T., Tomàs, F., Romero, J., 2011. Response of *Posidonia oceanica* to burial dynamics. Mar. Ecol. Prog. Ser. 423, 27–38. https://doi.org/10.3354/meps08970.

Marbà, N., Duarte, C.M., 1994. Growth response of the seagrass *Cymodocea nodosa* to experimental burial and erosion. Mar. Ecol. Prog. Ser. 107, 307–311. https://doi.org/10.3354/meps107307.

Marbà, N., Duarte, C.M., 2010. Mediterranean warming triggers seagrass (*Posidonia oceanica*) shoot mortality. Glob. Change Biol. 16 (8), 2366–2375. https://doi.org/10.1111/j.1365-2486.2009.02130.x.

Marbà, N., Cebrián, J., Enríquez, S., Duarte, C.M., 1996. Growth patterns of Western Mediterranean seagrasses: Species-specific responses to seasonal forcing. Mar. Ecol. Prog. Ser. 133, 203–215. https://doi.org/10.3354/meps133203.

Marbà, N., Díaz-Almela, E., Duarte, C.M., 2014. Mediterranean seagrass (*Posidonia oceanica*) loss between 1842 and 2009. Biol. Conserv. 176, 183–190. https://doi.org/10.1016/j.biocon.2014.05.024.

Marco-Méndez, C., Marbà, N., Amores, A., Romero, J., Minguito-Frutos, M., García, M., et al., 2024. Evaluating the extent and impact of the extreme Storm Gloria on *Posidonia oceanica* seagrass meadows. Sci. Total Environ. 908, 168404. https://doi.org/10.1016/j.scitotenv.2023.168404.

Mateo, M.A., Romero, J., Pérez, M., Littler, M.M., Littler, D.S., 1997. Dynamics of millenary organic deposits resulting from the growth of the Mediterranean seagrass *Posidonia oceanica*. Estuar. Coast Shelf Sci. 44 (1), 103–110. https://doi.org/10.1006/ecss.1996.0116.

Mateo, M.Á., Renom, P., Michener, R.H., 2010. Long-term stability in the production of a NW Mediterranean *Posidonia oceanica* (L.) delile meadow. Palaeogeogr. Palaeoclimatol. Palaeoecol. 291 (3–4), 286–296. https://doi.org/10.1016/j.palaeo.2010.03.001.

Mazarrasa, I., Marbà, N., Lovelock, C.E., Serrano, O., Lavery, P.S., Fourqurean, J.W., Kennedy, H., Mateo, M.A., Krause-Jensen, D., Steven, A.D.L., Duarte, C.M., 2015. Seagrass meadows as a globally significant carbonate reservoir. Biogeosciences 12, 4993–5003. https://doi.org/10.5194/bg-12-4993-2015.

Mazarrasa, I., Samper-Villarreal, J., Serrano, O., Lavery, P.S., Lovelock, C.E., Marbà, N., et al., 2018. Habitat characteristics provide insights of carbon storage in seagrass meadows. Mar. Pollut. Bull. 134, 106–117. https://doi.org/10.1016/j.marpolbul.2018.01.059.

McDonald, A.M., McDonald, R.B., Cebrián, J., Sánchez Lizaso, J.L., 2023. Reconstructed life history metrics of the iconic seagrass *Posidonia oceanica* (L.) detect localized anthropogenic disturbance signatures. Mar. Environ. Res. 186, 105901. https://doi.org/10.1016/j.marenvres.2023.105901.

Monnier, B., Pergent, G., Mateo, M.Á., Carbonell, R., Clabaut, P., Pergent-Martini, C., 2021. Sizing the carbon sink associated with *Posidonia oceanica* seagrass meadows using very high-resolution seismic reflection imaging. Mar. Environ. Res. 170, 105415. https://doi.org/10.1016/j.marenvres.2021.105415.

Montefalcone, M., Vacchi, M., Archetti, R., Ardizzone, G., Astruch, P., Bianchi, C.N., et al., 2019. Geospatial modelling and map analysis allowed measuring regression of the upper limit of *Posidonia oceanica* seagrass meadows under human pressure. Estuar. Coast Shelf Sci. 217, 148–157. https://doi.org/10.1016/j.ecss.2018.11.006.

Napolitano, E., Carillo, A., Iacono, R., Struglia, M.V., dell'Aquila, A., Palma, M., et al., 2025. Unprecedented Mediterranean Sea warming in 2024: analysis of the driving mechanisms. Front. Mar. Sci. 12, 1668204. https://doi.org/10.3389/fmars.2025.1668204.

Nguyen, H.M., Ruocco, M., Dattolo, E., Cassetti, F.P., Calvo, S., Tomasello, A., Marín-Guirao, Procaccini, G., 2023. Signs of local adaptation by genetic selection and isolation promoted by extreme temperature and salinity in the Mediterranean seagrass *Posidonia oceanica*. Mol. Ecol. https://doi.org/10.1111/mec.17032. ISSN: 0962-1083.

Noè, S., Bellavia, C., Calvo, S., Mazzola, A., Pirrotta, M., Sciandra, M., Vizzini, S., Tomasello, A., 2020. Resilience of the seagrass *Posidonia oceanica* following pulse-type disturbance. Mar. Environ. Res. 159, 105011. https://doi.org/10.1016/j.marenvres.2020.105011.

Oprandi, A., Mucerino, L., De Leo, F., Bianchi, C.N., Morri, C., Azzola, A., et al., 2020. Effects of a severe storm on seagrass meadows. Sci. Total Environ. 748, 141373. https://doi.org/10.1016/j.scitotenv.2020.141373.

Pergent, G., Boudouresque, C.-F., Crouzet, A., Meinesz, A., 1989. Cyclic changes along *Posidonia oceanica* rhizomes (lepidochronology): present state and perspectives. Mar. Ecol. 10 (3), 221–230. https://doi.org/10.1111/j.1439-0485.1989.tb00474.x.

Pergent, G., Bazairi, H., Bianchi, C.N., Boudouresque, C.F., Buia, M.C., Calvo, S., et al., 2014. Climate change and Mediterranean seagrass meadows: a synopsis for environmental managers. Mediterr. Mar. Sci. 15 (2), 462–473. https://doi.org/10.12681/mms.621.

Pergent-Martini, C., Pergent, G., Monnier, B., Boudouresque, C.-F., Mori, C., Valette-Sansevin, A., 2021. Contribution of *Posidonia oceanica* meadows in the context of climate change mitigation in the Mediterranean Sea. Mar. Environ. Res. 165, 105236. https://doi.org/10.1016/j.marenvres.2020.105236.

Perzia, P., Falautano, M., Castriota, L., Cillari, T., Vivona, P., Toccaceli, M., et al., 2011. Indagine geomorfologica e bionomica dei fondali di Sciacca (AG). Biogeographia–J. Integr. Biogeogr. 30 (1). https://doi.org/10.21426/B630110552.

Potouroglou, M., Bull, J.C., Krauss, K.W., Kennedy, H.A., Fusi, M., Daffonchio, D., et al., 2017. Measuring the role of seagrasses in regulating sediment surface elevation. Sci. Rep. 7 (1), 11917. https://doi.org/10.1038/s41598-017-12354-y.

Romero, J., Pérez, M., Mateo, M.A., Sala, E., 1994. The belowground organs of the Mediterranean seagrass *Posidonia oceanica* as a biogeochemical sink. Aquat. Bot. 47 (1), 13–19. https://doi.org/10.1016/0304-3770(94)90044-2.

Salomidi, M., Katsanevakis, S., Borja, A., Braeckman, U., Damalas, D., Galparsoro, I., et al., 2012. Assessment of goods and services, vulnerability, and conservation status of European seabed biotopes: a stepping stone towards ecosystem-based marine spatial management. Mediterr. Mar. Sci. 13 (1), 49–88. https://doi.org/10.12681/mms.23.

Serrano, O., Mateo, M.A., Renom, P., Julià, R., 2012. Characterization of soils beneath a *Posidonia oceanica* meadow. Geoderma 185, 26–36. https://doi.org/10.1016/j.geoderma.2012.03.020.

Serrano, O., Ruhon, R., Lavery, P.S., Kendrick, G.A., Hickey, S., Masqué, P., et al., 2016. Impact of mooring activities on carbon stocks in seagrass meadows. Sci. Rep. 6, 23193. https://doi.org/10.1038/srep23193.

Tomasello, A., Calvo, S., Di Maida, G., Lovison, G., Pirrotta, M., Sciandra, M., 2007. Shoot age as a confounding factor on detecting the effect of human-induced disturbance on *Posidonia oceanica* growth performance. J. Exp. Mar. Biol. Ecol. 343 (2), 166–175. https://doi.org/10.1016/j.jembe.2006.11.017.

Tomasello, A., Sciandra, M., Muggeo, V.M.R., Pirrotta, M., Di Maida, G., Calvo, S., 2016. Reference growth charts for *Posidonia oceanica* seagrass: an effective tool for assessing growth performance by age and depth. Ecol. Indic. 69, 50–58. https://doi.org/10.1016/j.ecolind.2016.04.005.

Tomasello, A., Cassetti, F.P., Savona, A., Pampalone, V., Pirrotta, M., Calvo, S., Signa, G., Andolina, C., Mazzola, A., Vizzini, S., Muzirafuti, A., Lanza, S., Randazzo, G., 2020. The use of very high-resolution images for studying *Posidonia oceanica* reefs. Vie et Milieu – Life Environ. 70 (3-4), 25–35. https://hal.sorbonne-universite.fr/hal-03342412v1.

Tomasello, A., Signa, G., Cassetti, F.P., Rende, S.F., Cilluffo, G., Pampalone, V., Vizzini, S., 2025. Discovering a beach "cemetery" of a seagrass *Posidonia oceanica* barrier reef: search for clues to reconstruct its origins. Estuar. Coast Shelf Sci. 316, 109164. https://doi.org/10.1016/j.ecss.2025.109164.

Vassallo, P., Paoli, C., Rovere, A., Montefalcone, M., Morri, C., Bianchi, C.N., 2013. The value of the seagrass *Posidonia oceanica*: a natural capital assessment. Mar. Pollut. Bull. 75 (1–2), 157–167. https://doi.org/10.1016/j.marpolbul.2013.07.044.

Vizzini, S., 2009. Analysis of the trophic role of mediterranean seagrasses in marine coastal ecosystems: a review. Bot. Mar. 52 (5), 383–393. https://doi.org/10.1515/BOT.2009.056.